

Long-wavelength nonequilibrium optical phonon dynamics in cubic and hexagonal semiconductors

Saswati Barman and G. P. Srivastava*

School of Physics, University of Exeter, Stocker Road, Exeter EX4 4QL, United Kingdom

(Received 2 September 2003; revised manuscript received 7 January 2004; published 30 June 2004)

We have investigated the relaxation of zone-center nonequilibrium optical phonons in bulk cubic and hexagonal semiconductors. Our theory is based on the application of Fermi's golden rule formula involving anharmonic interaction between phonons. Calculations of the lifetimes of the zone-center longitudinal optical (LO) and transverse optical (TO) phonons in cubic materials have been performed by modeling acoustic phonon modes within Debye's isotropic continuum scheme. Lifetimes of $A_1(\text{LO})$, $E_1(\text{TO})$, $A_1(\text{TO})$, E_2^2 and E_2^1 modes in wurtzite semiconductors have also been calculated by employing Debye's scheme within a semi-isotropic continuum model for acoustic modes. We have obtained a few trends in the lifetime results within a crystal phase (cubic or hexagonal), and between the two crystal phases. Our results support and explain available experimental data over a large temperature range, and make some predictions.

DOI: 10.1103/PhysRevB.69.235208

PACS number(s): 63.20.Kr, 63.20.Dj

I. INTRODUCTION

Study of optical phonon relaxation in semiconductors is important because of its direct influence in energy relaxation of carriers. In technologically important devices electrons are highly excited into conduction band either optically or by applying electric field. These high energy carriers decay towards their ground state, largely by emission of optical phonons. When the excited carrier density is large, the optical phonon emission can be very fast with an eventual nonequilibrium population. The hot phonon population increases the phonon absorption rates of the carriers, eventually reducing their energy loss which strongly affects the optical characteristic and electronic transport properties of the semiconductor devices. Therefore, the thermal management in electronic devices is dominantly controlled by the nonequilibrium optical phonons created by the excited carriers. Such optical phonons occupy a limited and well defined range of wave vectors close to the center of the Brillouin zone.¹ In polar semiconductors excess energy of carriers is removed mainly by the interaction of longitudinal optical (LO) phonons with the carriers, known as the Fröhlich interaction.

The LO phonon damping in polar systems has been studied experimentally both in the frequency domain using spontaneous Raman spectroscopy,²⁻⁶ and in the time domain using incoherent anti-Stokes Raman scattering^{7,8} and time-resolved coherent anti-Stokes Raman scattering.⁹⁻¹¹ Transverse optical (TO) phonons are less important in carrier-lattice thermalization due to their weak coupling with carriers. In highly doped semiconductors carrier-LO phonon interaction is damped due to screening effect.¹² In this case TO phonons play an important role in the redistribution of energy in highly excited systems. Relaxation of TO phonons has been studied by several groups by applying time-resolved coherent anti-Stokes Raman scattering techniques.¹³⁻¹⁷ Most of such experimental studies have been reported for cubic semiconductors with the diamond and zinc blende structures. Recently, a few groups have reported measurements of the phonon relaxation of the Raman active modes in the wurtzite phase of GaN and AlN. However, interpretation of such experimental results is more involved

mainly due to the presence of nine optical modes in the wurtzite structure.

Relatively far fewer theoretical investigations have been reported in this field. In general, phonon dephasing in solids results from various sources like impurity scattering, carrier scattering, and anharmonic interaction between phonons. For high quality crystals with low concentration of free carriers ($<4 \times 10^{16}/\text{cm}^3$), phonon dephasing due to carrier-phonon scattering and impurity scattering can be neglected. Also, depopulation of nonequilibrium optical phonons takes place on the time scale of about 1 ps at room temperature,¹⁷ which is much larger than that due to carrier-phonon interaction (~ 100 fs).¹⁸ Therefore, we can safely assume that the lifetime of the hot phonons is almost exclusively contributed by anharmonic interactions in the form of decay into phonons of lower energies.

The first theoretical calculation of phonon lifetime was performed by Cowley in Ge way back in 1965.¹⁹ Cowley considered the anharmonic interaction as an axially symmetric force between nearest neighbors and summed over all possible decay processes. Klemens²⁰ treated the decay of optical phonons into two acoustic phonons with opposite wave vectors. Available theoretical estimates of phonon lifetimes for bulk semiconductors show a huge spread and are only partially successful in accounting for experimental findings. The first detailed calculations of anharmonic phonon decay with a clear understanding of different decay mechanisms has been done by Debernardi, Baroni, and Molinari.^{21,22} Following a first-principles approach to study anharmonic decay of phonons based on the electronic density functional theory, the lifetime of the zone-center phonon in diamond, Si, Ge was calculated by Debernardi and co-workers,²¹ and for the zone-center LO and TO phonons in GaAs, GaP, AlAs, InP by Debernardi.²²

In this work we present a comprehensive study of the anharmonic phonon lifetime in cubic and hexagonal semiconductors, and provide a detailed analysis of the various decay processes involved. We have employed a semiempirical approach for this purpose. Our model uses the lowest order anharmonicity as perturbation to the crystal harmonic

potential. The expression for the decay rate has been obtained by applying Fermi's golden rule formula in time dependent perturbation theory, with an expression for cubic anharmonicity obtained in the framework of isotropic continuum model. Calculations for cubic systems have been performed by modeling acoustic phonon modes within Debye's isotropic continuum scheme. Lifetimes of various optical modes in wurtzite semiconductors have also been calculated by employing Debye's scheme within a semi-isotropic continuum model. These results are used to support and explain available experimental data, and to make predictions in some other cases. Particular attention has been paid to the study of III-nitride materials in both zinc blende and wurtzite phases.

II. THEORY

During carrier relaxation in semiconductors, nonequilibrium phonons are generated with wave vectors very close to the Brillouin zone center. In this section we describe our theory of anharmonic decay of such phonons.

A. Hamiltonian and Fermi's golden rule

In reality, anharmonicity is only a small proportion of the total crystal Hamiltonian, and can thus be considered as a perturbation on the harmonic part of the potential. We treat only the lowest order anharmonicity and express the Hamiltonian as

$$H = H_{\text{harm}} + V_3, \quad (1)$$

where H , H_{harm} , and V_3 represent the total crystal potential, the harmonic part of the Hamiltonian, and the cubic anharmonic part of the potential, respectively. Even only with the cubic anharmonic term, the expression for the full crystal Hamiltonian is very complicated. We have used a form of V_3 from Ref. 23, which treats the crystal as an anharmonic elastic continuum. Although the continuum model does not support optical phonon modes, many previous works have used such a model (see, e.g., Ref. 24). In this approach the cubic anharmonic part of the crystal Hamiltonian, using the second quantized notation, is expressed as²³

$$V_3 = \frac{1}{3!} \sqrt{\frac{\hbar^3}{8\rho^3 N_0 \Omega}} \sum_{\mathbf{q}, \mathbf{q}', \mathbf{q}''} \sqrt{\frac{qq'q''}{c_s c_{s'} c_{s''}}} A_{qq'q''}^{ss's''} \delta_{\mathbf{q}+\mathbf{q}'+\mathbf{q}'', \mathbf{G}} \times (a_{\mathbf{q}_s}^\dagger - a_{-\mathbf{q}_s})(a_{\mathbf{q}'_{s'}}^\dagger - a_{-\mathbf{q}'_{s'}})(a_{\mathbf{q}''_{s''}}^\dagger - a_{-\mathbf{q}''_{s''}}), \quad (2)$$

where ρ is the material density, N_0 is the number of unit cells, Ω is the volume per unit cell, q, q', q'' are the wave vectors of phonons with polarization indices s, s', s'' , and speeds $c_s, c_{s'}, c_{s''}$, respectively, $A_{qq'q''}^{ss's''}$ is a measure of the strength of a phonon-phonon scattering process, \mathbf{G} is a reciprocal lattice vector, and $a_{\mathbf{q}_s}^\dagger, a_{\mathbf{q}_s}$ are the phonon creation and annihilation operators. Strictly speaking, there is no concept of a reciprocal lattice vector for a continuum, but a drafting technique can be used (cf. Ref. 23 and references therein).

The probability of a three-phonon interaction from an initial state $|i\rangle$ to a final state $|f\rangle$ can be expressed, within Fermi's golden rule formula, as

$$P_i^f = \frac{2\pi}{\hbar} |\langle f | V_3 | i \rangle|^2 \delta(E_f - E_i). \quad (3)$$

While the lifetime of a mode \mathbf{q}_s is determined from the balance between the decay process $\mathbf{q}_s \rightarrow \mathbf{q}'_{s'} + \mathbf{q}''_{s''}$ and the fusion process $\mathbf{q}_s + \mathbf{q}'_{s'} \rightarrow \mathbf{q}''_{s''}$, it has been shown previously²⁵ that the fusion process is usually too slow, indicating that the lifetime is almost exclusively governed by the decay process. In the single-mode relaxation time approach,²³ we assume that phonons in mode \mathbf{q}_s are in non-equilibrium population while phonons in modes $\mathbf{q}'_{s'}$ and $\mathbf{q}''_{s''}$ maintain their equilibrium Bose-Einstein distribution. Within this concept, and using Eqs. (2) and (3), the decay rate of a phonon in mode \mathbf{q}_s can be expressed as

$$\tau_{\mathbf{q}_s}^{-1} = \frac{\pi \hbar \gamma^2}{2\rho \bar{c}^2 N_0 \Omega} \sum_{\mathbf{q}'_{s'}, \mathbf{q}''_{s''}} \omega(\mathbf{q}_s) \omega(\mathbf{q}'_{s'}) \omega(\mathbf{q}''_{s''}) \frac{\bar{n}_{\mathbf{q}'_{s'}} \bar{n}_{\mathbf{q}''_{s''}}}{\bar{n}_{\mathbf{q}_s}} \times \delta_{\mathbf{q}, \mathbf{q}'+\mathbf{q}''} \delta(\omega(\mathbf{q}_s) - \omega(\mathbf{q}'_{s'}) - \omega(\mathbf{q}''_{s''})), \quad (4)$$

where $\omega(\mathbf{q}_s)$ is the frequency of mode \mathbf{q}_s with the equilibrium Bose-Einstein distribution function $\bar{n}(\mathbf{q}_s)$, \bar{c} is the average acoustic phonon speed, and the three-phonon interaction strength $|A_{qq'q''}^{ss's''}|^2$ for the process $\mathbf{q}_s \rightarrow \mathbf{q}'_{s'} + \mathbf{q}''_{s''}$ has been expressed in the form²³

$$|A_{qq'q''}^{ss's''}|^2 = \frac{4\rho^2}{\bar{c}^2} \gamma^2 c_s^2 c_{s'}^2 c_{s''}^2, \quad (5)$$

with γ as the mode-average Grüneisen's constant. In general, γ is a wave vector, polarization mode, and temperature dependent. For the present study, however, we need to consider the value of γ for the LO and TO modes at the zone center (i.e., for $\mathbf{q}=0$). We will consider a temperature-average value of these coefficients. Furthermore, in this work we will regard $\gamma(\text{LO})$ and $\gamma(\text{TO})$ as adjustable parameters and consider different interaction coefficients $|A_{qq'q''}^{ss's''}|^2$ for different three-phonon processes in accordance with Eq. (5). Such an approach for the consideration of the anharmonic coupling constant to fit the temperature dependence of experimental lifetimes of phonons is a common practice.²⁶

B. Model dispersion curves

Measurements and realistic calculations of phonon dispersion relations for zinc blende and wurtzite materials are well documented. For example, the phonon dispersion curves for GaN can be found in Refs. 27 and 28 for the wurtzite phase and in Ref. 29 for both the zinc blende and wurtzite phases. In the long wavelength limit acoustic curves can be approximated by linear dispersion relations. Although the optical branch of a diatomic linear chain can be approximated by a quadratic dispersion relation, dispersion relations of three-dimensional crystals are in general quite complicated and a simple approximation is not always possible.

To derive analytical expressions for the decay rate of a zone-center optical mode due to cubic anharmonicity in the crystal potential, we made appropriate approximations for phonon dispersion curves for zinc blende and wurtzite mate-

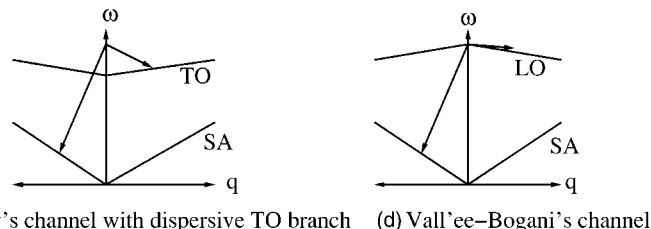
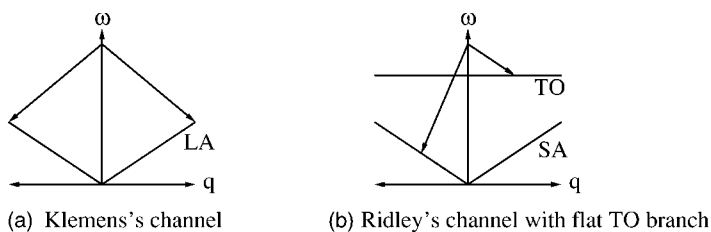


FIG. 1. Schematic illustration of our model dispersion curves for zinc blende materials.

rials. We used the Debye model within the continuum approximation for acoustic branches, and considered optical branches as flat or linearly (rather than quadratically) dispersive as appropriate. For diamond and zinc blende materials we further employed the isotropic approximation. A schematic illustration of our model dispersion curves for zinc blende materials has been presented in Fig. 1. For the wurtzite structure, we employed the Debye model within a semi-isotropic model. In this scheme our calculations were performed along the three principal symmetry directions $\Gamma-K$, $\Gamma-M$ and $\Gamma-A$, and results were presented as the average of the values along these directions. A schematic illustration of the modeled dispersion relations for the wurtzite structure is presented in Fig. 2. It should be noted that the quadratical variation with frequency of the density of states obtained from the application of the linear dispersion relation is in general quite different from that obtained from the consideration of realistic phonon dispersion relations. This should be kept in mind when critically analyzing the results presented in this work.

C. Expressions for intrinsic lifetime

A long wavelength optical phonon mode can decay into lower energy optical and/or acoustic modes dictated by en-

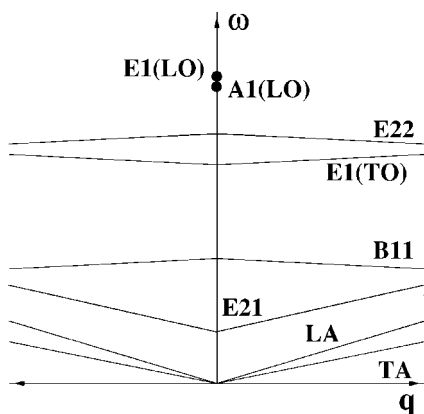


FIG. 2. Schematic illustration of our model dispersion curves for wurtzite materials.

ergy and momentum conservation conditions. It is convenient to describe such a decay in terms of four possible channels. (i) The decay of the optical phonon into two acoustic phonons with opposite momenta is known as the Klemens channel.²⁰ (ii) Ridley³⁰ considered the possibility of a zone-center longitudinal optical mode decaying into a transverse optical mode and a longitudinal acoustic mode. This can be generalized to a process involving the decay of the optical mode into a lower-branch optical mode and an acoustic mode: we shall call this a generalized Ridley channel. (iii) The optical mode may decay into a lower mode of the same branch and an acoustic mode, known as the Vallée-Bogani channel.^{9,10} (iv) In addition to the above three channels, in wurtzite materials a zone-center optical mode may also decay into two lower-branch optical modes. Within the Debye model for phonon dispersion, as briefly described above, we have derived the following expressions for phonon intrinsic lifetime:

(a) *Klemens channel:*

$$\tau^{-1}[\text{SO} \rightarrow \text{S}'\text{A} + \text{S}''\text{A}] = \frac{\hbar \gamma^2}{64 \pi \rho \bar{c}^2 c_{S'A}^3} \omega_{\text{SO}}^5 \frac{[\bar{n}(\omega_{\text{SO}}/2)]^2}{\bar{n}(\omega_{\text{SO}})}, \tag{6}$$

$$\begin{aligned} \tau^{-1}[\text{SO} \rightarrow \text{S}'\text{A} + \text{S}''\text{A}] &= \frac{\hbar \gamma^2}{4 \pi \rho \bar{c}^2 c_{S''A}^3} \omega_{S''A}^3 \omega_{\text{SO}} \omega_{S'A} \frac{\bar{n}(\omega_{S'A}) \bar{n}(\omega_{S''A})}{\bar{n}(\omega_{\text{SO}})}, \end{aligned} \tag{7}$$

(b) *Generalized Ridley channel:*

$$\begin{aligned} \tau^{-1}[\text{SO} \rightarrow \text{S}'\text{O} + \text{S}''\text{A}] &= \frac{\hbar \gamma^2}{4 \pi \rho \bar{c}^2 c_{S''A}^3} \omega_{S''A}^3 \omega_{\text{SO}} \omega_{S'O} \frac{\bar{n}(\omega_{S'O}) \bar{n}(\omega_{S''A})}{\bar{n}(\omega_{\text{SO}})}, \end{aligned} \tag{8}$$

(c) *Generalized Vallée-Bogani channel:*

$$\begin{aligned} & \tau^{-1}[\text{SO} \rightarrow \text{SO}^{\text{edge}} + S''\text{A}] \\ &= \frac{\hbar \gamma^2}{4\pi\rho\bar{c}^2 c_{S''\text{A}}^3} \omega_{S''\text{A}}^3 \omega_{\text{SO}} \omega_{\text{SO}}^{\text{edge}} \frac{\bar{n}(\omega_{\text{SO}}^{\text{edge}}) \bar{n}(\omega_{S''\text{A}})}{\bar{n}(\omega_{\text{SO}})}, \quad (9) \end{aligned}$$

(d) *Further channels:*

$$\begin{aligned} & \tau^{-1}[\text{SO} \rightarrow S'\text{O} + S''\text{O}] \\ &= \frac{\hbar \gamma^2}{4\pi\rho\bar{c}^2 c_{S''\text{O}}^3} \omega_{S''\text{O}}^3 \omega_{\text{SO}} \omega_{S'\text{O}} \frac{\bar{n}(\omega_{S'\text{O}}) \bar{n}(\omega_{S''\text{O}})}{\bar{n}(\omega_{\text{SO}})}, \quad (10) \end{aligned}$$

where $S, S', S''=L$ or T , ω^{edge} is zone-edge frequency, and $\omega_{S''\text{A}} = \omega_{\text{SO}} - \omega_{S'\text{O}}$ or $\omega_{\text{SO}} - \omega_{\text{SO}}^{\text{edge}}$, and $\omega_{S''\text{O}} = \omega_{\text{SO}} - \omega_{S'\text{O}}$. Processes involving daughter modes from optical branches, referred to as “further channels,” can take place in wurtzite materials, but not in materials with the diamond and zinc blende structures.

D. Possible decay channels

Energy and momentum conservation conditions may allow for the zone-center LO and TO phonon modes in zinc blende materials to decay via one or many of the Klemens, Ridley and Vallée-Bogani channels. In particular, the following combinations of daughter modes may be allowed:³¹

LO mode decay:

- (i) Klemens channel: $\text{LO} \rightarrow \text{LA} + \text{LA}; \text{LA} + \text{TA}; \text{TA} + \text{TA}$,
- (ii) Ridley channel: $\text{LO} \rightarrow \text{TO} + \text{LA}; \text{TO} + \text{TA}$,
- (iii) Vallée-Bogani channel: $\text{LO} \rightarrow \text{LO}(\text{zone edge}) + \text{LA}; \text{LO}(\text{zone edge}) + \text{TA}$.

TO mode decay:

- Klemens channel: $\text{TO} \rightarrow \text{LA} + \text{LA}; \text{LA} + \text{TA}; \text{TA} + \text{TA}$.

In wurtzite materials there are several zone-center optical modes: $A_1(\text{LO}), E_2^2, E_1(\text{TO}), A_1(\text{TO})$, and E_2^1 . Decay of the $A_1(\text{LO})$ mode is allowed via channels (a) (Klemens), (b) (Ridley), and (d) (Further) involving daughter modes $B_1^1, B_1^2, E_2^2, E_2^1, E_1(\text{TO}), A_1(\text{TO})$ and acoustic modes. Modes $E_1(\text{TO}), E_2^2$, and $A_1(\text{TO})$ are also allowed to decay via channels (a), (b), and (d). Only the Klemens channel is allowed for the decay of E_2^1 .

III. RESULTS AND DISCUSSIONS

We will present results for a number of materials in the (hexagonal) wurtzite structure, and a number of materials in the (cubic) zinc blende and diamond structures. We will also compare results for a few nitride materials which may be grown in both wurtzite and zinc blende structures. We used the material density ρ , characteristic phonon frequencies, phonon acoustic speeds, and γ as listed in Landolt-Börnstein,³² unless otherwise stated. When considering decay via further channels, for simplicity we considered the phonon speed in low-lying daughter optical branches as half of the longitudinal acoustic speed.

A. Wurtzite structure

In this section we will present results for the decay rate of various optical modes in III-nitride materials InN, GaN, AlN, and BN in the wurtzite phase. The results for individual materials will be used to obtain useful trends. Group theoretical analysis³³ suggests that while the modes A_1, E_2 , and E_1 are Raman active, the mode B_1 is silent. With this information in mind, we have made calculations of the lifetimes of only A_1, E_2 , and E_1 modes. As mentioned earlier, calculations were performed along the three symmetry directions $\Gamma-K, \Gamma-M$, and $\Gamma-A$, and the final decay result for each mode is presented as an average of the results along these directions. The computed estimates are compared with available experimental measurements.

Our calculated lifetime at low temperature and room temperature, along with available experimental data from Raman scattering measurements and time-resolved spontaneous Raman scattering technique, are reported in Table I. There is lack of information on Grüneisen’s constant γ for different modes in the various nitrides. The recent work by Bruls *et al.*³⁴ suggests that for AlN the value of γ between 300 and 1600 K lies in the range 0.70 and 0.96. In this work, we used $\gamma=0.8$ (the average of results reported in Bruls *et al.*³⁴ for 300 and 1600 K) for all modes in all the nitride materials discussed here, unless otherwise discussed further in the text. Any rescaling of γ to fit theory with experiment becomes necessary in the absence of any reliable experimental data for different modes, and also in view of the simplified dispersion relation employed.

I. InN

$A_1(\text{LO})$ mode. An examination of the phonon dispersion curves of InN,²⁹ with the help of Fig. 2, indicates that the $A_1(\text{LO})$ mode can decay via the Ridley and “further” channels. In particular, we find that the following Ridley decay processes take place:

$$\begin{aligned} & A_1(\text{LO}) \rightarrow E_2^2 + \text{TA}; A_1(\text{LO}) \rightarrow E_2^2 + \text{LA}; \\ & A_1(\text{LO}) \rightarrow E_1(\text{TO}) + \text{LA}; A_1(\text{LO}) \rightarrow E_1(\text{TO}) + \text{TA}; \\ & A_1(\text{LO}) \rightarrow A_1(\text{TO}) + \text{LA}; A_1(\text{LO}) \rightarrow A_1(\text{TO}) + \text{TA}. \end{aligned}$$

In addition, the following “further” decay processes are allowed:

$$\begin{aligned} & A_1(\text{LO}) \rightarrow E_2^2 + E_2^1; A_1(\text{LO}) \rightarrow E_1(\text{TO}) + E_2^1; \\ & A_1(\text{LO}) \rightarrow A_1(\text{TO}) + E_2^1. \end{aligned}$$

Along $\Gamma-K$ all these decay mechanisms are allowed, along $\Gamma-M$ only the second of Ridley processes, and all the “further” processes are allowed, and along $\Gamma-A$ (the c direction) only the “further” processes are allowed. Our calculated lifetime values are 0.19 ps at 5 K (low temperature) and 0.08 ps at 300 K. It is found that “further” channels contribute very strongly (about 80%) towards the decay process. In particular, the last two processes listed above provide a contribution of about 60%.

E_2^2 mode. The E_2^2 mode can follow the Ridley mechanism to decay into $E_1(\text{TO}) + (\text{TA}, \text{LA})$, and $A_1(\text{TO}) + (\text{TA}, \text{LA})$

TABLE I. Calculated lifetime (τ) results of the zone-center optical phonons in wurtzite materials at 6 K (LT) and 300 K (RT). These results were obtained with the choice $\gamma=0.8$ for the mode-averaged Grüneisen's constant. For comparison, available experimental results are also given.

Mode	Material	Lifetime (ps)			
		LT		RT	
		Theory	Expt.	Theory	Expt.
$A_1(\text{LO})$	InN	0.19		0.08	
	GaN	3.0	5.0 ^a	1.5	3.0, ^a 0.62–1.16 ^b
	AlN	0.27	0.75 ^d	0.16	0.57, ^d 0.45 ^c
	BN	0.1		0.08	
E_2^2	InN	30.4		3.3	
	GaN	2.2		1.3	1.4 ^c
	AlN	1.52	2.9 ^d	0.89	0.83 ^c
	BN	0.34		0.27	
$E_1(\text{TO})$	InN				
	GaN	2.3		1.4	0.95 ^c
	AlN	0.8		0.46	0.91 ^c
	BN	0.1		0.08	
$A_1(\text{TO})$	InN				
	GaN	1.2		0.7	0.4 ^c
	AlN	0.73		0.41	0.76 ^c
	BN	0.15		0.12	
E_2^1	InN	252.2		25.21	
	GaN	507		81.7	10.1 ^c
	AlN	44.0		11.2	4.4 ^c
	BN	14.9		7.3	

^aReference 35.

^bReference 36.

^cReference 37.

^dReference 38.

along both Γ -M and Γ -K. Along Γ -A there is no participation from the LA mode in the above processes. The total lifetime decreases from 30.4 ps at 5 K to 3.3 ps at room temperature. At 300 K, the percentage contributions of the processes $E_2^2 \rightarrow E_1(\text{TO}) + \text{TA}$ and $E_2^2 \rightarrow A_1(\text{TO}) + \text{TA}$ are 41% and 51%, respectively.

E_2^1 mode. E_2^1 is the lowest optical mode. Therefore, only acoustic branches are available as the daughter modes. All of the possible three processes $E_2^1 \rightarrow \text{TA} + \text{TA}$, $E_2^1 \rightarrow \text{LA} + \text{LA}$, $E_2^1 \rightarrow \text{LA} + \text{TA}$ fulfill the energy and momentum conservation conditions. The calculated low temperature and room temperature values of the lifetime are 252.2 and 25.21 ps, respectively. At room temperature the relative weight of the processes $E_2^1 \rightarrow \text{TA} + \text{TA}$ and $E_2^1 \rightarrow \text{LA} + \text{TA}$ are 84% and 14.5%, respectively.

2. GaN

$A_1(\text{LO})$ mode. The decay of the zone-center $A_1(\text{LO})$ mode in GaN can only take place via Ridley's channel. The various combinations of daughter phonon modes involved in such decay processes are:

- (i) $A_1(\text{LO}) \rightarrow E_2^2 + \text{LA}$; (ii) $A_1(\text{LO}) \rightarrow E_1(\text{TO}) + \text{LA}$;
- (iii) $A_1(\text{LO}) \rightarrow E_2^2 + \text{TA}$; (iv) $A_1(\text{LO}) \rightarrow E_1(\text{TO}) + \text{TA}$;
- (v) $A_1(\text{LO}) \rightarrow B_1^1 + \text{LA}$; (vi) $A_1(\text{LO}) \rightarrow B_1^1 + \text{TA}$.

However, an examination of the phonon dispersion curves²⁹ shows that processes (i)–(iv) are not allowed along Γ -A, process (ii) is not allowed along Γ -M, and process (v) is not allowed along Γ -K. Our computed results give a very slow decay rate for processes (v) and (vi) in the three symmetry directions. Similarly, along Γ -K and Γ -M directions processes (iii) and (iv) give much smaller lifetime than the other processes, thus providing the main contribution.

The total lifetime decreases from 3.0 ps at 6 K to 1.5 ps at 300 K. The lifetime of this mode has been measured by Tsen *et al.*³⁵ and by Tripathy, Chua, and Ramam.³⁶ On the other hand, Bergman *et al.*³⁷ did not manage to measure the lifetime of this mode due to heavy plasmon damping effect. Using metalorganic chemical vapor deposition grown *n*-doped GaN sample Tripathy and co-workers estimated the room temperature value of the lifetime in the range

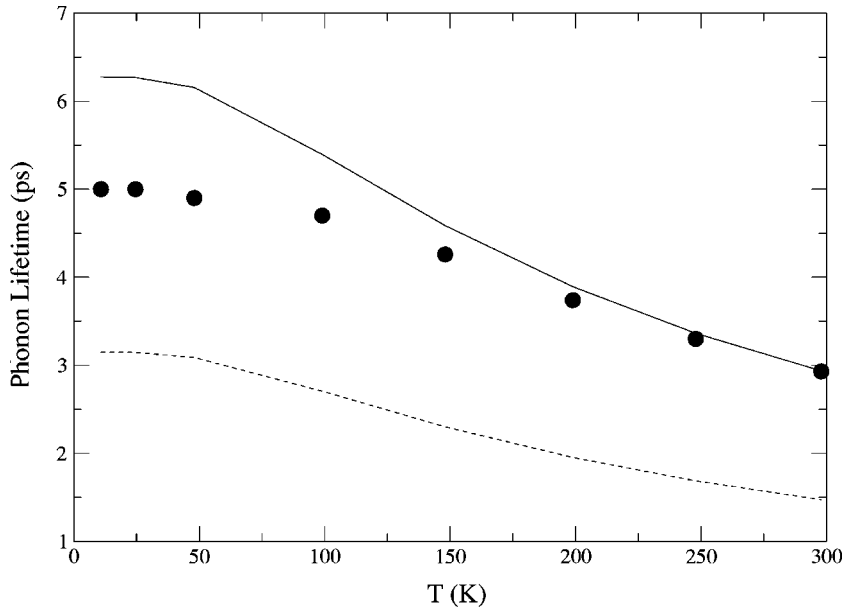


FIG. 3. Temperature variation of the lifetime of the $A_1(\text{LO})$ mode in wurtzite AlN. The solid and dashed curves are obtained with the Grüneisen's constant γ taken as 0.57 and 0.8, respectively. Filled circles represent experimental data from Tsen *et al.* (see Ref. 35).

0.62–1.16 ps from their measured Raman linewidth under different processing conditions such as wet chemical treatment, rapid thermal annealing, and thermal annealing. Tsen *et al.*³⁵ measured the lifetime values of 5 and 3 ps at low temperature and room temperature, respectively, by employing time-resolved spontaneous Raman spectroscopy for molecular beam epitaxy grown undoped samples. The theoretical estimate by Ridley³⁰ for low temperature decay rate of $5.0 \times 10^{11} \text{ s}^{-1}$ corresponds to the lifetime value of 2 ps. As seen in Fig. 3 the temperature variation of the lifetime from our theoretical work agrees very well with the experimental measurements by Tsen *et al.*³⁵ beyond 150 K. The theoretical result can be matched to the experimental value at room temperature by scaling down the Grüneisen constant γ to 0.57. However, with the scaled value of γ the theoretical curve lies appreciably above the experimental data points for temperatures below 150 K. We believe that the difference between theory and experiment can be explained by incorporating contributions from additional scattering processes which do not depend on temperature. Possible sources would be boundary, isotope, and impurity scatterings. Although it is relatively straightforward to compute such contributions, we have not made an attempt to include contributions from such scatterings.

The dominant contribution ($\sim 60\%$) in limiting the $A_1(\text{LO})$ phonon lifetime is its decay into a $E_1(\text{TO})$ mode and a TA mode. The next important contribution ($\sim 30\%$) comes from the decay into a E_2^2 mode and a TA mode. Processes (i) and (ii) with daughter modes as E_2^2 or $E_1(\text{TO})$ and a LA have almost negligible contribution. In analyzing their data Tsen *et al.*³⁵ have concluded that the $A_1(\text{LO})$ mode decays most effectively into a large wave vector TO phonon and a large wave vector LA or TA phonon. Our work agrees with this analysis but provides a more accurate description of the most possible decay mechanism.

E_2^2 , $E_1(\text{TO})$, and $A_1(\text{TO})$ modes. The zone-center energies of the E_2^2 , $E_1(\text{TO})$, and $A_1(\text{TO})$ modes are very close to each other. These optical modes can possibly decay into two lower

energy optical modes [a “further” channel as described in Eq. (10)], or one optical and one acoustic mode (Ridley's channel). Relaxation of these modes via Klemens's channel is forbidden on account of the energy and momentum conservation requirements. The resulting decay mechanisms for E_2^2 mode are

$$(i) E_2^2 \rightarrow E_1(\text{TO}) + \text{TA}; \quad (ii) E_2^2 \rightarrow A_1(\text{TO}) + \text{TA};$$

$$(iii) E_2^2 \rightarrow B_1^1 + E_2^1.$$

Of these three, the first two processes are found to contribute very little (less than 5% at room temperature) towards the lifetime of the E_2^2 mode. While the third process is not allowed along the c axis, its contributions along the in-plane directions make up to 97% of the total lifetime result. It is found that the lifetime of this mode is slightly lower than that of the $A_1(\text{LO})$ mode. The computed room-temperature result of 1.3 ps (obtained with the unscaled value of $\gamma=0.8$) is in good agreement with the experimental measurement of 1.4 ps.³⁷

Although there are two possible decay channels for $E_1(\text{TO})$: (i) $E_1(\text{TO}) \rightarrow A_1(\text{TO}) + \text{TA}$, and (ii) $E_1(\text{TO}) \rightarrow B_1^1 + E_2^1$, from our calculations we find that almost 100% contribution to the total decay rate comes from $E_1(\text{TO}) \rightarrow B_1^1 + E_2^1$. The numerical values of the calculated lifetime for these modes are 2.3 and 1.4 ps at low and room temperatures, respectively. The room-temperature value of the experimental measurement³⁷ of this mode is 0.95 ps, which is about 1.5 times smaller than our calculated result.

The only possible decay channel for $A_1(\text{TO})$ mode is $A_1(\text{TO}) \rightarrow B_1^1 + E_2^1$. Similar to the E_2^2 and $E_1(\text{TO})$ modes, this mode does not decay along the Γ -A direction (c axis). The computed lifetime values for this mode are 1.2 and 0.7 ps at 6 and 300 K, respectively. The experimental measurement³⁷ gives a lifetime value of 0.4 ps at room temperature.

E_2^1 mode. E_2^1 is the lowest energy optical mode in the hexagonal GaN. The only available decay channel for this

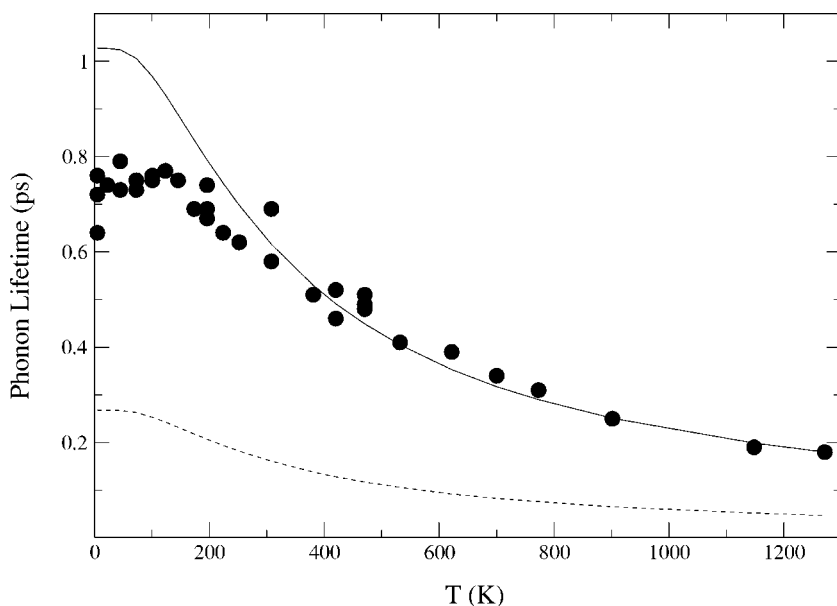


FIG. 4. Temperature variation of the lifetime of the $A_1(\text{LO})$ mode in wurtzite AlN. The solid and dashed curves are obtained with the Grüneisen's constant γ taken as 0.41 and 0.8, respectively. Filled circles represent experimental data from Kuball *et al.* (see Ref. 38).

mode is the Klemens channel. The decay processes for this mode are $E_2^1 \rightarrow \text{LA} + \text{TA}$, $E_2^1 \rightarrow \text{TA} + \text{TA}$, and $E_2^1 \rightarrow \text{LA} + \text{LA}$. These processes are allowed along the three principal symmetry directions. Our calculations, however, suggest that this mode is very long lived, with a lifetime at least ten times that of the other optical modes. The long-lived nature of this mode is in agreement with the experimental results obtained by Bergman *et al.*³⁷ who reported 10.1 ps for the room-temperature lifetime of this mode.

3. AlN

$A_1(\text{LO})$ mode. The allowed decay processes for the $A_1(\text{LO})$ mode in AlN are (i) $A_1(\text{LO}) \rightarrow B_1^2 + \text{TA}$; (ii) $A_1(\text{LO}) \rightarrow B_1^2 + \text{LA}$; (iii) $A_1(\text{LO}) \rightarrow E_2^2 + \text{TA}$; (iv) $A_1(\text{LO}) \rightarrow E_2^2 + \text{LA}$; (v) $A_1(\text{LO}) \rightarrow E_1(\text{TO}) + \text{LA}$; (vi) $A_1(\text{LO}) \rightarrow A_1(\text{TO}) + \text{TA}$; (vii) $A_1(\text{LO}) \rightarrow A_1(\text{TO}) + \text{LA}$; (viii) $A_1(\text{LO}) \rightarrow E_2^2 + E_2^1$. However, along the c axis only $A_1(\text{LO}) \rightarrow B_1^2 + \text{TA}$, $A_1(\text{LO}) \rightarrow B_1^2 + \text{LA}$, $A_1(\text{LO}) \rightarrow E_2^2 + E_2^1$ processes contribute. The decay mechanisms $A_1(\text{LO}) \rightarrow E_2^2 + E_2^1$ and $A_1(\text{LO}) \rightarrow E_1(\text{TO}) + \text{LA}$ are absent along Γ -M and Γ -K directions, respectively. The relative main contributions of various processes are found as follows: $A_1(\text{LO}) \rightarrow A_1(\text{TO}) + \text{TA}$ (35%), $A_1(\text{LO}) \rightarrow E_2^2 + \text{TA}$ (23%), $A_1(\text{LO}) \rightarrow B_1^2 + \text{TA}$ (15%), and $A_1(\text{LO}) \rightarrow E_2^2 + E_2^1$ (16%) over the entire temperature range. The rest of the total contribution comes from other Ridley-like processes.

Kuball *et al.*³⁸ measured lifetime values of 0.75 and 0.57 ps at 10 K and room temperature, respectively. Bergman *et al.*³⁷ measured the lifetime value of 0.45 ps at room temperature by employing a micro Raman scattering technique. The lower of the two experimental values reported in the work by Bergman *et al.* is possibly due to more impurities in their samples. Notwithstanding the difference between the values reported by the two experimental groups, there is a fundamental difference in the manner they have analyzed their results. While Bergman *et al.* explained the decay of the $A_1(\text{LO})$ mode to occur via Ridley's channel into a large wave

vector TO mode and an LA mode, Kuball *et al.*³⁸ analyzed their results on the basis of Klemens's model. An inspection of the phonon dispersion curves for AlN in Ref. 29 clearly suggests that due to substantial mass difference between the Al and the N atoms, there exists a large gap between the acoustic and optical phonon branches in the AlN phonon spectrum, with the $A_1(\text{LO})$ frequency at Γ point being 910 cm^{-1} , and at the zone-edge LA frequency being 314 cm^{-1} . So, similar to the case of the $A_1(\text{LO})$ decay in GaN, Klemens's model is not applicable for the decay of this mode in AlN, since $2\omega_{\text{LA}} < \omega_{\text{LO}}$. As reported above, the Ridley-type processes give rise to a massive contribution of 84% and further channels with two optical daughter modes contribute approximately 16%.

For the choice $\gamma=0.8$, our computed values for the $A_1(\text{LO})$ mode lifetime are 0.27 and 0.16 ps at low temperature and room temperature, respectively. These values are much lower than those measured from Raman linewidth by Kuball *et al.* and Bergman *et al.* In order to improve agreement between our theoretical results and the experimental results of Kuball *et al.*, we scaled Grüneisen's constant down to $\gamma=0.41$. This was done to match theory with experiment at the highest reported temperature in the experimental data. This was considered to be more sensible than fitting the experimental results at the low-temperature end in view of the fact that extra, temperature-independent, scattering mechanisms are likely to contribute at low temperatures. Figure 4 shows the theoretical results, and their comparison with the experimental data by Kuball *et al.*,³⁸ for the entire temperature range covered in their experimental work. Clearly the theory explains the magnitude and temperature dependence of the experimental data all the way down to 300 K. However, below about 200 K, the theoretical curve lies appreciably above the experimental data points. In view of the fact that the experimental data below 200 K are rather temperature insensitive, we suggest that the role of extra mechanisms, such as boundary and impurity scatterings, should be included in explaining the experimental data.

E_2^2 mode. An inspection of the phonon dispersion curves

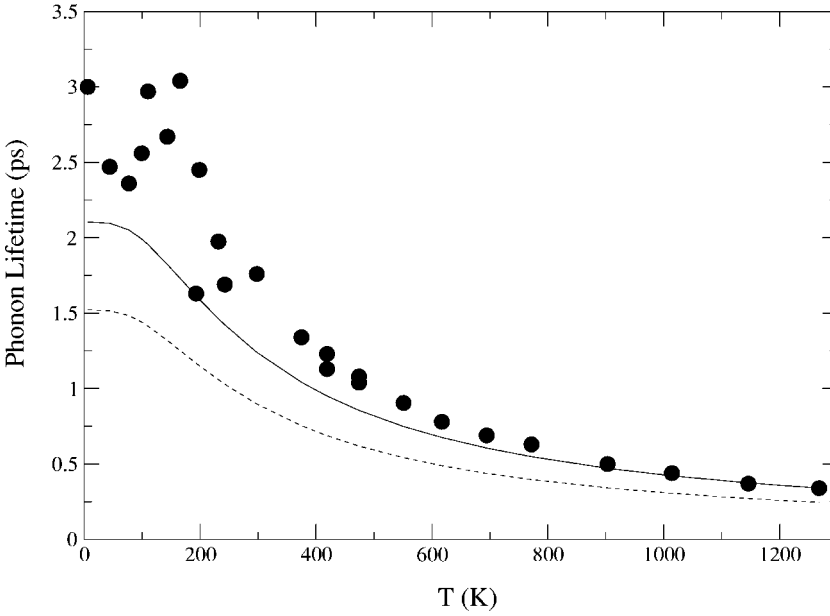


FIG. 5. Temperature variation of the lifetime of the E_2^2 mode in wurtzite AlN. The solid and dashed curves are obtained with the Grüneisen's constant γ taken as 0.68 and 0.8, respectively. Filled circles represent experimental data from Kuball *et al.* (see Ref. 38).

reported in Ref. 29 shows the energetically possible decay mechanisms for the E_2^2 mode are $E_2^2 \rightarrow E_1(\text{TO}) + \text{TA}$, $E_2^2 \rightarrow E_1(\text{TO}) + \text{LA}$, $E_2^2 \rightarrow A_1(\text{TO}) + \text{TA}$, $E_2^2 \rightarrow A_1(\text{TO}) + \text{LA}$, $E_2^2 \rightarrow B_1^1 + \text{TA}$, $E_2^2 \rightarrow B_1^1 + \text{LA}$, $E_2^2 \rightarrow E_2^1 + \text{TA}$, $E_2^2 \rightarrow E_2^1 + \text{LA}$, and $E_2^2 \rightarrow B_1^1 + E_2^1$. We find that the most dominant decay routes are $E_2^2 \rightarrow E_2^1 + \text{TA}$ ($\sim 60\%$) and $E_2^2 \rightarrow B_1^1 + E_2^1$ ($\sim 20\%$) over the entire temperature range. Figure 5 shows the variation of the lifetime over a large temperature range. With the choice of $\gamma=0.8$, our calculations produce lifetime values of 1.52, 0.89, and 0.25 ps at low temperature, room temperature, and 1200 K, respectively. Our room-temperature result is in good agreement with the Raman measurement of 0.83 ps (Ref. 37) on a high quality sample. At the high-temperature end our theoretical results agree quite well with the measurements reported by Kuball *et al.*³⁸ A scaled down value of $\gamma=0.68$ brings the theoretical curve in very good agreement with the experimental data³⁸ in the temperature range 400–1200 K. Although there is a marked scatter in the experimental data at low temperatures, we note that the theoretical curve falls slightly below the experimental data. For example, at 10 K the experimental value reported by Kuball *et al.* is 2.9 ps, whereas we obtain 2.1 ps. This is in contrast to the low temperature results for the lifetime of the $A_1(\text{LO})$ mode, for which the theoretical curve lies above the experimental data. Boundary and impurity scatterings are likely to reduce the theoretical result even further down. We suggest that a different value of γ , larger than its high-temperature magnitude, would be helpful in explaining the low-temperature experimental results.

$E_1(\text{TO})$ mode. The processes which contribute to the decay of the $E_1(\text{TO})$ mode are $E_1(\text{TO}) \rightarrow A_1(\text{TO}) + \text{TA}$, $E_1(\text{TO}) \rightarrow A_1(\text{TO}) + \text{LA}$, $E_1(\text{TO}) \rightarrow B_1^1 + \text{TA}$, $E_1(\text{TO}) \rightarrow B_1^1 + \text{LA}$, $E_1(\text{TO}) \rightarrow E_2^1 + \text{TA}$, $E_1(\text{TO}) \rightarrow E_2^1 + \text{LA}$, $E_1(\text{TO}) \rightarrow B_1^1 + E_2^1$, $E_1(\text{TO}) \rightarrow \text{LA} + \text{LA}$. Our calculations yield the lifetime values of 0.8 ps at 5 K and 0.46 ps at 300 K. The process $E_1(\text{TO}) \rightarrow E_2^1 + \text{TA}$ provides the main contribution ($\sim 60\%$). The next important contribution comes from the process $E_1(\text{TO}) \rightarrow B_1^1 + \text{TA}$ ($\sim 15\%$). The only available experimental

measurement is by Bergman *et al.* who reported 0.91 ps at room temperature via Raman spectroscopy.³⁷ No attempt was made to improve agreement between theory and experiment.

$A_1(\text{TO})$ mode. The decay channels available for the decay of the $A_1(\text{TO})$ mode are: $A_1(\text{TO}) \rightarrow B_1^1 + \text{TA}$, $A_1(\text{TO}) \rightarrow B_1^1 + \text{LA}$, $A_1(\text{TO}) \rightarrow E_2^1 + \text{TA}$, $A_1(\text{TO}) \rightarrow E_2^1 + \text{LA}$, $A_1(\text{TO}) \rightarrow B_1^1 + E_2^1$, $A_1(\text{TO}) \rightarrow \text{LA} + \text{LA}$. Along the c axis only $A_1(\text{TO}) \rightarrow B_1^1 + \text{LA}$ and $A_1(\text{TO}) \rightarrow B_1^1 + E_2^1$ processes are allowed. Along the Γ -M direction the allowed processes are $A_1(\text{TO}) \rightarrow B_1^1 + \text{TA}$, $A_1(\text{TO}) \rightarrow B_1^1 + \text{LA}$, $A_1(\text{TO}) \rightarrow E_2^1 + \text{TA}$ and $A_1(\text{TO}) \rightarrow E_2^1 + \text{LA}$, and along the Γ -K direction the allowed process is $A_1(\text{TO}) \rightarrow B_1^1 + \text{TA}$. The most important decay mechanism in limiting the lifetime is $A_1(\text{TO}) \rightarrow E_2^1 + \text{TA}$, contributing approximately 80%. Our findings for the lifetime values are 0.73 ps at 5 K and 0.41 ps at 300 K. These values are lower than the experimentally measured lifetime value of 0.76 ps³⁷ at 300 K. Again, no attempt was made to improve agreement between the theory and experiment.

E_2^1 mode. E_2^1 is the lowest lying optical mode in AlN, with the zone-center frequency lower than the zone-edge TA frequencies. So, the available daughter modes are only the acoustic branches close to the zone center. Along Γ -K direction only the $E_2^1 \rightarrow \text{TA} + \text{TA}$ process contributes. At room temperature, the processes $E_2^1 \rightarrow \text{TA} + \text{TA}$ and $E_2^1 \rightarrow \text{LA} + \text{TA}$ contribute 86% and 14%, respectively. The total lifetime is 44 ps at low temperature reducing to 11.2 ps at room temperature. The reported room-temperature lifetime value from the Raman scattering measurements is 4.4 ps.³⁷ Similar to GaN, the lifetime of the E_2^1 mode is relatively longer than that of other modes.

4. BN

$A_1(\text{LO})$ mode. BN is the only wurtzite material considered here for which the $A_1(\text{LO})$ mode can decay via three channels: Klemens, Ridley, and further. Compatible with the energy-momentum conservation conditions, the $A_1(\text{LO})$ mode in BN can decay via Ridley's channel into one of the

optical modes ($E_1(\text{TO}), A_1(\text{TO}), E_2^2, B_1^1$) and an acoustic mode, via Klemens's channel into two LA modes, and via "further" channels into a combination of B_1^1 and E_2^1 . Not all of these processes are, however, allowed in all of the three principal symmetry directions $\Gamma-A$, $\Gamma-M$, and $\Gamma-K$. The most important contribution (about 30%) comes from the process $A_1(\text{LO}) \rightarrow E_2^1 + \text{TA}$. Another 40% is almost equally contributed by the processes $A_1(\text{LO}) \rightarrow E_1(\text{TO}) + \text{TA}$, $A_1(\text{LO}) \rightarrow A_1(\text{TO}) + \text{TA}$, and $A_1(\text{LO}) \rightarrow B_1^1 + \text{TA}$. The remaining 30% contribution comes from the other allowed processes. The overall contributions from Klemens's, Ridley's, and "further" channels are 5%, 70%, and 25%, respectively. Our calculations suggest very short lifetime values of 0.1 and 0.08 ps at low temperature and room temperature, respectively. To the best of our knowledge there is no report of any experimental measurement of phonon lifetimes in hexagonal BN.

$E_1(\text{TO})$, $A_1(\text{TO})$ and E_2^2 modes. These modes can decay via Ridley's, Klemens's, and "further" channels. Along $\Gamma-A$ some of these processes are, however, not allowed. For the $E_1(\text{TO})$ mode we computed lifetime values of 0.1 ps at low temperature and 0.08 ps at room temperature, with main contributions from the processes $E_1(\text{TO}) \rightarrow E_2^1 + E_2^1$ (48%), $E_1(\text{TO}) \rightarrow \text{TA} + \text{TA}$ (23%), and $E_1(\text{TO}) \rightarrow \text{LA} + \text{TA}$ (15%). The calculated lifetime results for the $A_1(\text{TO})$ mode are 0.15 ps at low temperature and 0.12 ps at room temperature, with main contributions from $A_1(\text{TO}) \rightarrow E_2^1 + E_2^1$ (50%) and $A_1(\text{TO}) \rightarrow \text{TA} + \text{TA}$ (20%). The phonon lifetime of the E_2^2 mode decreases from 0.34 ps at low temperature to 0.27 ps at 300 K. The relative weights of the processes are 50% from $E_2^2 \rightarrow E_2^1 + E_2^1$, 20% from $E_2^2 \rightarrow \text{TA} + \text{TA}$, and 12% from $E_2^2 \rightarrow B_1^1 + \text{TA}$.

E_2^1 mode. The mode E_2^1 can decay via Klemens's channel into two TA modes, or into a combination of LA and TA modes, along $\Gamma-A$ and $\Gamma-M$ (but not along $\Gamma-K$). The decay into a pair of TA modes gives almost the total contribution (92%). This is the longest-lived mode, with a total lifetime value of 14.9 ps at low temperature and 7.3 ps at room temperature.

5. Comparisons and trends

The results presented above indicate that there are no regular trends for the lifetimes of optical modes across the nitride materials. It seems that the $E_1(\text{TO})$ and $A_1(\text{TO})$ modes in InN do not decay at all. For other materials the E_2^1 mode is the longest lived. The lifetime of the lowest lying optical mode, E_2^2 , is at least an order of magnitude longer than that of the other modes in all of the chosen wurtzite materials. The shortest-lived mode in InN and AlN is $A_1(\text{LO})$, in BN are $A_1(\text{LO})$ and $E_1(\text{TO})$, and in GaN it is $A_1(\text{TO})$. For any mode, the shortest lifetime occurs for BN. Experimental results for GaN and AlN are supportive of our theoretical results.

It is interesting to note that the lifetime of the highest optical mode, $A_1(\text{LO})$, in GaN is roughly an order of magnitude larger than in the other nitrides. There is some support for this behavior from experimental measurements on GaN and AlN. While the decay of the $A_1(\text{LO})$ mode is dominated

by the Ridley channel in GaN, AlN, and BN, it is more strongly controlled by "further" channels in InN. On the other hand, the Klemens channel is disallowed in all nitrides, except BN for which it makes only a minor contribution. Our work also indicates that the lifetime of the E_2^2 , $E_1(\text{TO})$, and $A_1(\text{TO})$ modes decrease across InN, GaN, AlN, BN.

The decay of the lowest lying optical mode E_2^1 in all of these materials is dominantly controlled by the Klemens mechanism where the daughter phonons are two TA phonons with equal and opposite momenta. For the E_2^2 , $E_1(\text{TO})$, $A_1(\text{TO})$ modes in GaN, the decay probability is maximum via the "further" decay channel involving B_1^1 and E_2^1 phonon modes. In AlN these modes primarily decay via the Ridley channel, with the daughter modes being E_2^1 and TA. The dominant channel for these modes in BN involves two E_2^1 branches.

B. Diamond and zinc blende structures

In diamond structure materials the zone-center optical LTO mode can decay via Klemens's and Vallée-Bogani's channels. In zinc blende materials the LO mode can decay via Klemens's, Ridley's, and Vallée-Bogani's channels, and the TO mode can only decay via Klemens's channel. In this section we present results of the lifetimes of the zone-center phonon modes in diamond and several zinc blende semiconductors. The results will be used to examine trends across different materials with the same crystal structure, and between the zinc blende and wurtzite phases of a given material. Our calculated results are presented, and compared with experiment, in Table II.

1. Diamond

In diamond the zone-center optical mode can only decay through the Klemens channel. Our calculations show that the phonon lifetime of the LTO mode is dominantly (90% contribution) controlled by its decay into different acoustic branches. The experimental determination by Zouboulis and Grimsditch³⁹ of the phonon lifetime from Raman linewidth suggests a value of 2.46 ps at room temperature. To explain their observation Zouboulis and Grimsditch also used the Klemens model. Using $\gamma=0.8$ we calculated the lifetime values of 2.54 ps at low temperature and 2.30 ps at room temperature. As seen from Fig. 6 our calculated results show good agreement over the entire temperature range of measurements made by Zouboulis and Grimsditch.

2. InN

The decay of the LO mode in cubic InN takes place solely via Ridley's channel. The processes $\text{LO} \rightarrow \text{TO} + \text{TA}$ and $\text{LO} \rightarrow \text{TO} + \text{LA}$ contribute 75% and 25%, respectively. The calculated values of the lifetime are 0.5 and 0.21 ps at low temperature and room temperature, respectively.

3. GaN

In GaN the zone-center LO phonon energy is too high for the Klemens channel to be allowed. Similarly, the Vallée-Bogani channel is not allowed. Therefore, the decay of the

TABLE II. Lifetime (τ) of the zone-center longitudinal optical phonon in diamond and zinc blende materials, together with relative contributions from various decay channels. Available experimental results are also presented. See text for the choice of the anharmonicity coefficient γ .

	τ (ps)		Klemens's channel (%)	Ridley's channel (%)	Vallée-Bogani channel (%)
	Present theory	experiment			
Low temperature (6 K)					
InN	0.5			100	
GaN	4.4			100	
AlN	0.45		30	70	
BN	0.44		82	18	
GaAs	8.7	16.5, ^a 9.2, ^b 8.5 ^f	66	8	26
InP	39.3	24.1[a], ^a 40.0 ^c		100	
AlSb	224.0			100	
HgSe	28.0		90	10	
Diamond	2.54		100		
Room temperature					
InN	0.21			100	
GaN	2.5			100	
AlN	0.32		30	70	
BN	0.39	1.45 ^e	77	23	
GaAs	2.3	2.1, ^c 2.39 ^f	52	15	33
InP	6.1	7.6, ^c 6.65 ^f		100	
AlSb	21.0			100	
HgSe	4.7		80	20	
Diamond	2.30	2.46 ^d	100		

[a] at 10 K.

^aReference 6.

^bReference 9.

^cReference 10.

^dReference 39.

^eReference 41.

^fReference 43.

LO mode can only take place via the Ridley channel, with more important contribution coming from the decay involving TA modes rather than LA modes. It should be pointed out that we considered the same value of the anharmonic coefficient ($\gamma=0.8$) for the cubic GaN as for the hexagonal phase. The calculated lifetime values are 4.4 and 2.5 ps at low temperature and room temperature, respectively. To the best of our knowledge, there is no report of any experimental measurement to compare our results.

4. AlN

In AlN the LO mode decays via both Ridley's and Klemens's channels, with 70% and 30% contributions, respectively. The dominant contribution (60%) is from the decay via Ridley's process $LO \rightarrow TO+TA$. The Klemens channel is only allowed for the process $LO \rightarrow LA+LA$. The low- and room-temperature lifetime values are calculated as 0.45 and 0.32 ps, respectively.

5. BN

Due to nearly equal cationic and anionic masses the phonon spectrum of cubic BN, similar to GaAs, shows no clear

separation between its optical and acoustic branches.⁴⁰ The zone-center LO mode can decay via the Ridley and Klemens channels. Our calculations suggest that the strongest contribution (about 75%) comes from the Klemens channel into $TA+TA$, and a reasonable contribution (about 20%) comes from the Ridley channel into $TO+TA$. The TO mode can only decay via the Klemens channel. We estimate contributions of 50% from the decay into $LA+TA$, 40% from the decay into $LA+LA$, and 10% from the decay into $TA+TA$. The lifetime values at low (room) temperature are 0.44 (0.39) and 1.68 (1.42) ps for the LO and TO modes, respectively. Table III lists our calculated values of the LO and TO lifetimes at three different temperatures, together with experimental results. At all temperature the lifetime of the TO mode is nearly four times the lifetime of the LO mode.

The calculated lifetime values are plotted against temperature in Fig. 7, where experimental measurements from Ref. 41 are also reproduced for comparison. For the TO mode the agreement between theory and experiment is very good for the magnitude and variation of the lifetime over the entire temperature range of the measurement. There is also very good agreement between theory and experiment for the

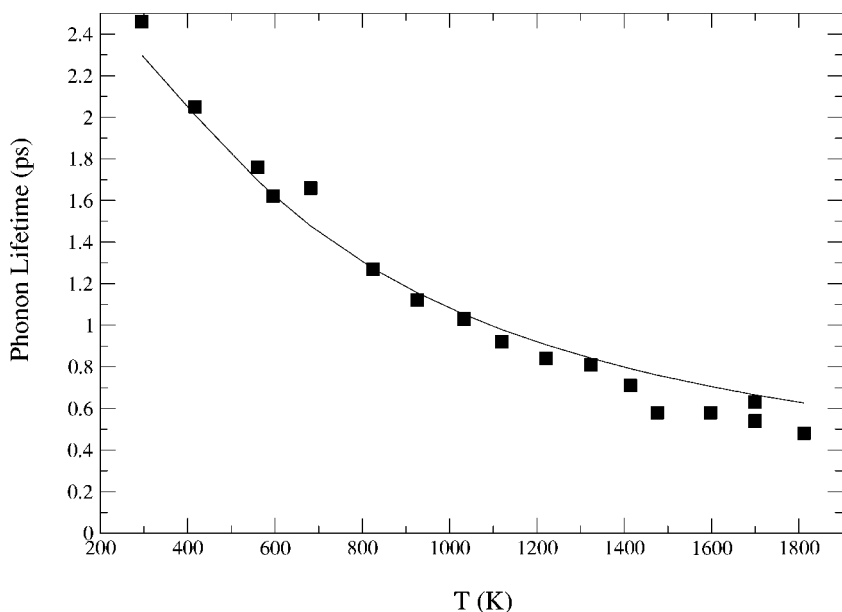


FIG. 6. Temperature variation of the lifetime of the LTO mode in diamond. Also shown are the experimental data taken from Zouboulis and Grimsditch (see Ref. 39).

lifetime results of the LO mode at the high-temperature end of the measurements. Surprisingly, the theoretical curve falls far below the experimental data at temperatures below 1300 K. In this respect we note that both the theoretical results and the experimental data show a linear temperature increase of the lifetime of the TO mode from the Debye temperature Θ_D (1700 K) down to $2/3 \Theta_D$. The same must be expected for the LO mode. Whereas this is vindicated from our theoretical results, the experimental data in Ref. 40 show that this behavior does not hold near $2/3 \Theta_D$.

It is interesting to note that the three-phonon linewidth fitted by Herchen and Cappelli⁴¹ to pass through the room-temperature datum could not fit the high-temperature end of

the data. If their theoretical fitting is shifted to match the high-temperature end of the data, the resulting lifetime result would fall very significantly below their experimental data points, as our results suggest. We should further point out that in their paper Herchen and Cappelli state that “the intensity of the anti-Stokes component of the LO mode was insufficient to record reliable spectra below 1200 K.” We are thus of the opinion that the experimental data at temperatures much below Θ_D may not be accurate and should be reinvestigated. We also do not share the view expressed by Herchen and Cappelli that higher order anharmonic processes would need to be taken into account to bring theoretical results close to experiment. This is because it is well documented

TABLE III. Lifetime (τ) results for the zone-center LO and TO phonon modes in InP, GaAs and cubic BN. The values of Grüneisen’s constant used are $\gamma(\text{LO})=1.24$, $\gamma(\text{TO})=1.24$ for InP; $\gamma(\text{LO})=1.8$, $\gamma(\text{TO})=1.8$ for GaAs; and $\gamma(\text{LO})=0.8$, $\gamma(\text{TO})=0.8$ for BN.

		Lifetime (ps)					
		Low temperature (6 K)		Low temperature (78 K)		Room temperature (300 K)	
		Present theory	experiment	Present theory	experiment	Present theory	experiment
InP	LO	39.3	24.18, ^a 40.0 ^d	19.1	22.0, ^d 34.5 ^g	6.1	7.6, ^d 6.65 ^g
	TO	11.0		9.7	12.0 \pm 1.5, ^e 10.7 \pm 1.1 ^g	3.9	2.6 \pm 0.4, ^e 2.5 ^g
GaAs	LO	8.7	16.5, ^a 9.2, ^c 8.5 ^g	6.4	6.4, ^d 6.25 ^b	2.3	2.1, ^d 2.39 ^g
	TO	8.3	7.1, ^g 6.2 ^e	6.9	\sim 5.0 ^e	2.5	2.3 ^g
BN	LO	0.44		0.44		0.39	1.45 ^f
	TO	1.68		1.68		1.42	1.6 ^f (at 271.5 K)

^aReference 6.

^bReference 7.

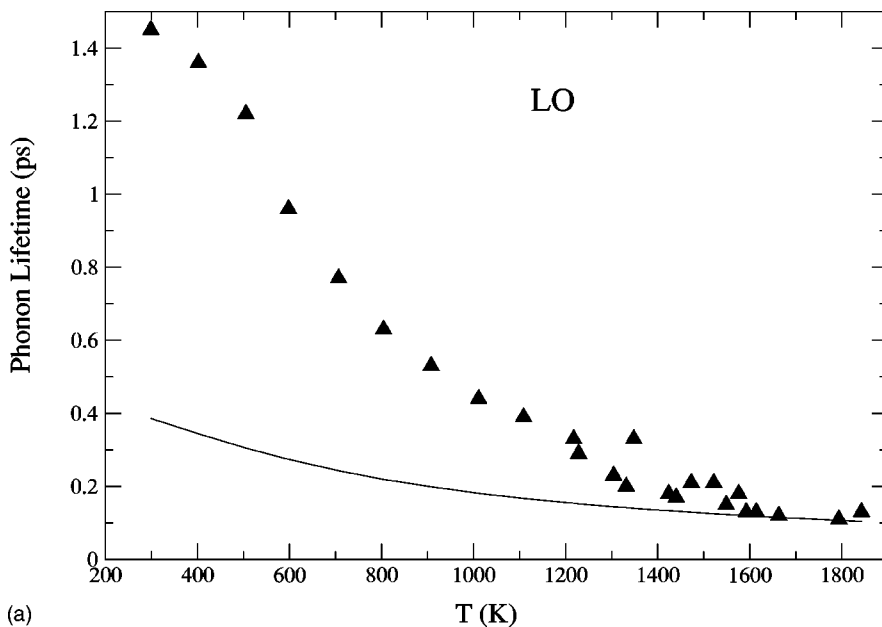
^cReference 9.

^dReference 10.

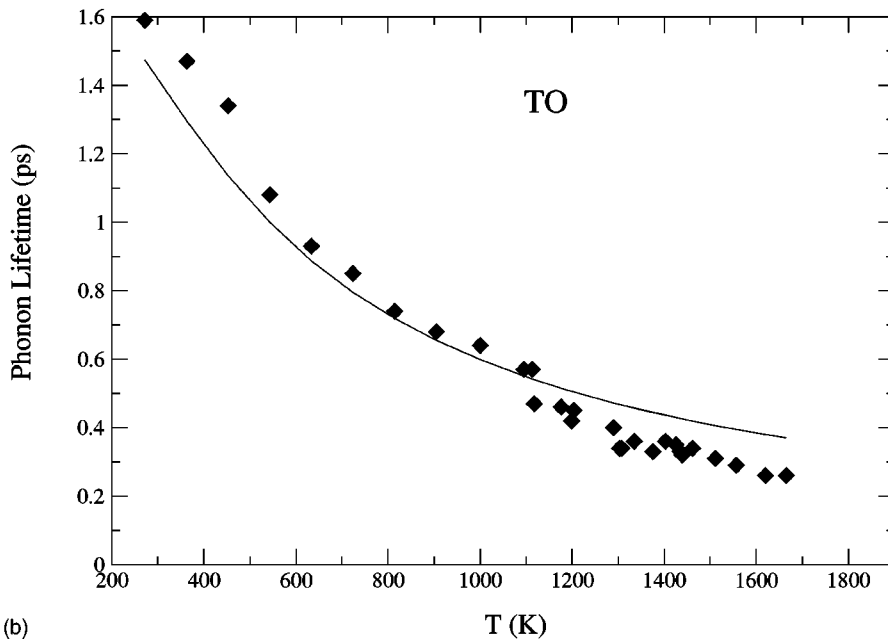
^eReference 12.

^fReference 41.

^gReference 43.



(a)



(b)

FIG. 7. Temperature variation of the lifetime of the LO and TO modes in cubic BN. Also shown are the experimental data taken from Herchen and Cappelli (see Ref. 41).

that in general four-phonon processes are at least two orders of magnitude weaker than three-phonon processes even at very large temperatures.⁴³

6. GaAs

The phonon spectrum of GaAs shows a downward dispersion of the LO branch.²⁹ This allows, subject to energy and momentum conservation rules, the decay of the zone-center LO phonon via the Vallée-Bogani channel into a zone-edge LO phonon and a TA phonon. Our calculations show that the Vallée-Bogani channel is quite important in the entire temperature range of our study. We find that the percentage contributions towards the total lifetime from the Klemens, Vallée-Bogani, and Ridley channels are 66%, 26%, and 8% at low temperatures, and 52%, 33%, and 15% at room temperature, respectively. The total phonon lifetime values are

8.7 and 2.3 ps at low and room temperatures, respectively. Our low and room temperature results, and the temperature dependence of the lifetime, agree well with the experimental measurements by Kash and Tsang⁸ and by Vallée and Bogani.^{9,10} Our work also strongly supports the view expressed in the works by Vallée and Bogani^{9,10} that the intraband combination relaxation process $LO \rightarrow LO' + TA$ is quite important in GaAs. However, our result for the Klemens channel is very different from Vallée's work. Our low-temperature result also agrees well with the previous theoretical result of 8.0 ps obtained by Debernardi.²² However, our findings for the percentage contributions of different channels are very different from Debernardi's work. Whereas Debernardi's work shows that the most important decay mechanism involves two different acoustic branches, we find that this mechanism does not fulfill the energy-momentum con-

servation condition. The main reason for the discrepancy with respect to the relative importance of different decay mechanisms between this work and the theoretical works by Vallée and by Debernardi is likely to be the simplified treatment of the density of states for acoustic branches in our work.

For the decay of the zone-center TO mode in GaAs, we find that the processes $\text{TO} \rightarrow \text{LA} + \text{LA}$ and $\text{TO} \rightarrow \text{LA} + \text{TA}$ are involved. Our calculations suggest that the lifetime of the TO mode is similar to that of the LO mode, with the low and high-temperature values for the TO mode lifetime being 8.3 and 2.5 ps, respectively. The process involving two different acoustic modes gives a higher contribution (59%) than the other process (41%) at room temperature. Our calculated lifetime values are in excellent agreement with the results obtained by Irmer, Wenzel, and Monecke⁴³ using the near-infrared Raman spectroscopy, who obtained lifetime values of 7.1 and 2.3 ps at low and room temperatures, respectively. Similarly, our results are in good agreement with the infrared time-resolved coherent anti-stokes Raman scattering measurements made by Ganikhanov and Vallée¹² of 6.2 and 1.5 ps at low and room temperatures, respectively. However, the two experimental groups have analyzed their measurements differently. In analyzing their data, Ganikhanov and Vallée clearly mentioned that the relaxation process is governed by the decay into acoustic modes involving two different branches, whereas Irmer, Wenzel, and Monecke proposed the decay mechanism involving two LA phonons. As mentioned earlier, our work clearly suggests that both of the abovementioned processes are almost equally important.

7. *AlSb*

In AlSb, similar to GaN, the LO branch lies too high for the zone-center mode to decay via Klemens's channel. Thus this is another material in which the LO phonon lifetime is solely controlled by Ridley's channel. For this material the Grüneisen constant is reported³² as $\gamma = 1.27$. Using this value we have calculated the total lifetime values of 224, 72, and 21 ps at 6, 77, and 300 K, respectively. These values are very large compared to other diamond and zinc blende materials we have studied. The contributions from the $\text{LO} \rightarrow \text{TO} + \text{TA}$ and $\text{LO} \rightarrow \text{TO} + \text{LA}$ processes are 80% and 20%, respectively.

8. *InP*

A discussion of results for the decay rates of the LO and TO modes in InP requires a critical examination of its dispersion curves in the acoustic range. We first note that there are fewer experimental data points for acoustic modes around the X symmetry point.⁴⁴ In particular, theoretical values for the LA frequency at the X point, obtained from the applications of the phenomenological bond charge model⁴⁵ as well as the first-principles density-functional theory,²² are appreciably lower than the experimental value.⁴⁴

The Klemens decay channel $\text{LO} \rightarrow \text{LA} + \text{LA}$ along the principal symmetry direction $\Gamma - X$ is allowed if the experimental result for the LA mode at X is accepted. However, this channel is completely disallowed on account of theoret-

ical prediction of the dispersion of the LA branch in the $\Gamma - X$ direction. Furthermore, both experimental and theoretical dispersion results clearly indicate that the Klemens channel $\text{LO} \rightarrow \text{LA} + \text{LA}$ is forbidden along the other two principal symmetry directions (viz., along $\Gamma - L$ and $\Gamma - K$). All other polarization combinations of the Klemens channel are completely forbidden. We have, therefore, based upon theoretical dispersion curves, disallowed the Klemens channel in InP altogether. The Vallée-Bogani channel is also disallowed in InP. Thus the decay of the LO mode is totally governed by Ridley's channel. The results of our calculations for the decay rates of the zone-center LO and TO modes are presented in Tables II and III. Our results are in very good agreement with the work by Debernardi²² who has shown that the decay of the LO mode is almost totally (99%) contributed by the Ridley channel, with only 1% contribution from the Klemens channel. Both the present work and the work by Debernardi seem to disagree with the work by Vallée,¹⁰ who has analyzed the relaxation of the LO mode either only in terms of the Klemens channel, or using almost identical contributions from the Klemens and the Ridley channels.

By using the value $\gamma = 1.24$ ³² for the Grüneisen constant, we have obtained the lifetime for the LO phonon as 39.3, 19.0, and 6.1 ps at 6, 78, and 300 K, respectively. Raman measurements carried out by Vallée¹⁰ give 40, 22, and 7.6 ps at 6, 78, and 300 K, respectively. Clearly, our results are in good agreement with Vallée's measurements at all these temperatures. Our room-temperature result is also in good agreement with the Raman measurement of 6.65 ps obtained by Irmer and co-workers.⁴³ However, it should be pointed out that there is some scatter in experimental results made at low temperatures. For example, at 78 K experimental measurements of 34.5 ps obtained by Irmer and co-workers is much larger than 22 ps obtained by Vallée. Similarly, the result (24.1 ps) obtained at 10 K by Kernohan *et al.*⁶ is much lower than the result (40 ps) obtained by Vallée. The low-temperature result of 139.7 ps obtained in the theoretical work by Debernardi²² seems to be too large compared to both our results as well as the existing experimental measurements.

For calculating the decay rate of the TO mode we used the same value of γ as for the LO mode, viz. $\gamma = 1.24$. This choice is reasonable, as the experimental values of γ for the zone-center LO and TO modes are quite similar.³² On account of energy conservation, the decay of the TO mode can only take place via the Klemens channel $\text{TO} \rightarrow \text{LA} + \text{LA}$. Our calculated values of the lifetime are 11.0, 9.7, and 3.9 ps at 6, 78, and 300 K, respectively. These results agree well with the Raman measurements carried out by Irmer and co-workers⁴³ and Ganikhanov and Vallée,¹² as well as with the low-temperature theoretical result obtained by Debernardi.²² We also note that the lifetime of the TO mode is smaller than the lifetime of the LO mode at all temperatures.

9. *HgSe*

HgSe is the only group II-VI material for which we have calculated the LO phonon lifetime. The reason for considering this material was that it has two characteristic features in

TABLE IV. Comparison of decay rates (τ^{-1}) of the zone-center $A_1(\text{LO})$ phonon in wurtzite materials and the LO mode in zinc blende materials at low and room temperatures. Temperature-average relative contributions from the Klemens, Ridley, and “further” channels are also presented.

	Decay rate (THz)		Klemens's channel (%)	Ridley's channel(%)	“Further” channels (%)
	6 K	300 K			
Zinc blende					
LO					
InN	2.0	4.8		100	
GaN	0.23	0.4		100	
AlN	2.2	3.1	30	70	
BN	2.3	2.6	80	20	
Wurtzite					
$A_1(\text{LO})$					
InN	5.3	12.5		20	80
GaN	0.33	0.7		100	
AlN	3.7	6.3		84	16
BN	10.0	12.5	5	70	25

its phonon dispersion curves. Apart from GaN, this is the only zinc blende material for which the TO branch shows a significant amount of *upward* dispersion. Second, the TA branch shows a significant amount of dip towards the zone boundary. Our calculations, with a choice of $\gamma=1.0$, based on the theoretical results for phonon frequencies and velocities in Ref. 46, produce lifetime values of 28.0 ps at low temperature and 4.7 ps at room temperature. Klemens's channel contributes heavily (80%) towards the decay, with 20% contribution from Ridley's channel.

10. Comparisons and trends

The investigations reported in this work allow us to draw a few comparisons and trends for the lifetime of zone-center optical modes in zinc blende materials. These are a direct result of the characteristic features of the phonon dispersion relations in these materials. From the results presented in Tables II and III we note the following trends.

(i) First, among all the zinc blende materials studied here the longest lifetime value for the LO mode is obtained for AlSb. The shortest end of the lifetime values is obtained for the nitrides InN, AlN, and BN.

(ii) Second, the decay of the LO mode through Klemens's channel can be directly related to the ratio of the basis atoms in the zinc blende materials. For example, the Klemens channel is forbidden in InP, InN, GaN, and AlSb. This can be easily understood from the application of the diatomic linear chain model, from which the condition for the Klemens channel to be allowed on energy grounds is that the mass ratio of the constituent atoms does not exceed 3. The mass ratio in each of InP, InN, GaN, and AlSb is much larger than 3, and consequently there are clear grounds for the Klemens channel to be disallowed. On the other hand, in diamond (mass ratio of 1.0) the Klemens channel provides 100% contribution towards the decay of the optical mode.

(iii) Third, Ridley's channel provides an important con-

tribution to the decay of the LO mode in all zinc blende materials, *albeit* of different proportion for different materials. In particular, in InP, InN, GaN, and AlSb, Ridley's channel provides 100% contribution.

(iv) GaAs is the only material studied here for which Vallée-Bogani's channel provides an important contribution to the decay of the LO mode.

(v) For a given material, the lifetime of the TO can be smaller, similar, or larger than that of the LO mode. As an empirical observation we note that $\tau(\text{TO})$ is expected to be larger, similar, and smaller than $\tau(\text{LO})$ if the cation-anion mass ratio m_c/m_a is smaller, similar, and larger than unity, respectively.

(vi) Based on the lifetime values of the LO mode, III-N materials can be grouped into two classes: GaN with relatively larger lifetime (comparable to GaAs), and InN, AlN, and BN with much shorter lifetimes.

C. Comparison of results between zinc blende and wurtzite phases

We will draw a few useful comparisons of phonon lifetimes between the zinc blende and wurtzite phases by considering our results for the Group III-N materials. Table IV displays a comparison of decay rate of the LO mode in the zinc blende phase and the $A_1(\text{LO})$ mode in the wurtzite phase for these materials. For all the nitrides considered here the $A_1(\text{LO})$ mode has a lifetime which is smaller than the lifetime of the LO mode in the entire temperature range studied here. In our view, different factors contribute to this result.

While the decay of the LO mode in cubic InN is totally governed by the Ridley channel, the decay of the $A_1(\text{LO})$ mode in the wurtzite phase is dominated by “further” channels. Due to the availability of a large number of “further” channels, the lifetime of the $A_1(\text{LO})$ mode is 2.6 times shorter than the lifetime of the LO mode.

For GaN Ridley's channel provides 100% contribution for the decay of the LO mode in the zinc blende phase and also for the $A_1(\text{LO})$ mode in the wurtzite phase. However, due to the availability of many more optical branches in the wurtzite phase, the $A_1(\text{LO})$ mode decays via a larger number of Ridley's decay processes than does the LO mode in the cubic phase. Our calculations suggest that at room temperature the lifetime of the $A_1(\text{LO})$ mode is about 1.5 times shorter than that of the LO mode.

In AlN the Klemens channel plays an important role (30%) in the decay rate of the LO mode in the zinc blende phase. The crystal structure of the wurtzite phase modifies the acoustic branches in AlN such that the Klemens channel is no longer allowed, but "further" channels provide strong contribution to the decay rate of the $A_1(\text{LO})$ mode (15%). As a result, the lifetime of the $A_1(\text{LO})$ mode is approximately 1.8 times shorter than the lifetime of the LO mode.

In BN the Klemens channel plays the dominant role (80%) in the decay of the LO mode in the zinc blende phase. Due to the changes in the phonon dispersion curves for the two crystal phases, the Klemens channel plays only a minor role (5%), and the Ridley channel becomes slightly less important, while "further" channels provide significant contribution (25%) towards the decay of the $A_1(\text{LO})$ mode. As a result of these changes, the lifetime of the $A_1(\text{LO})$ mode is approximately 4.5 times shorter than the lifetime of the LO mode.

From the above discussion we note two important points regarding the importance of "further" channels in the wurtzite phase. (i) Although the elimination or reduction of the Klemens channel for AlN and BN in the wurtzite phase should lead to an increase in the lifetime of the $A_1(\text{LO})$ mode, this is offset much more heavily by the decay contribution from "further" channels. (ii) The presence of several optical branches has led the "further" channels to contribute much more strongly than the Ridley channel in the wurtzite phase of InN.

IV. SUMMARY

In this work we have computed the lifetime of optical phonons in diamond, and zinc blende and wurtzite semicon-

ductors. We have systematically studied the relative importance of different available channels for the decay of such modes. Our results are in good agreement with available experimental data for most materials, except for the temperature variation of the LO mode in cubic BN. Our work also provides reliable predictions where there is lack of experimental data.

LO mode in zinc blende materials: Klemens's channel is forbidden in materials with the cation-anion mass ratio larger than 3, such as InP, InN, GaN, and AlSb. Ridley's channel provides an important contribution to the decay in all zinc blende materials, *albeit* of different proportion for different materials. GaAs is the only material studied here for which Vallée-Bogani's channel provides an important contribution. III-N materials can be grouped into two classes: GaN with relatively larger lifetime (comparable to GaAs), and InN, AlN, and BN with much shorter lifetimes.

LO vs TO modes in zinc blende materials: Compared to the LO mode, the TO mode is predicted to be short lived, of similar lifetime, and long lived for materials with the cation-anion mass ratio larger, similar, and smaller than unity.

$A_1(\text{LO})$ mode in wurtzite materials: The lifetime in GaN is roughly an order of magnitude larger than in the other nitrides. While the decay of this mode is dominated by the Ridley channel in GaN, AlN, and BN, it is more strongly controlled by "further" channels in InN. The Klemens channel is disallowed in all nitrides, except BN for which it makes only a minor contribution.

$A_1(\text{LO})$ vs LO: In general, the lifetime of the $A_1(\text{LO})$ mode is smaller than the lifetime of the LO mode. This is due to an intricate balance between the reduction (or elimination) of the contribution from the Klemens channel, reduction in the contribution from the Ridley channel, and development of the contribution from "further" channels in the wurtzite phase. GaN is, however, an exception for which the Ridley channel provides 100% contribution for the decay of the LO mode in the zinc blende phase and also for the $A_1(\text{LO})$ mode in the wurtzite phase.

Among the III-nitrides in the wurtzite phase, the shortest lifetime of any mode occurs for BN. The E_2^1 mode is the longest lived, by at least an order of magnitude compared to any other optical mode.

*Corresponding author.

¹J. Kash, J. Hvam, J. C. Tsang, and T. Kuech, Phys. Rev. B **38**, 5776 (1988).

²R. K. Chang, J. M. Ralston, and D. E. Keating, in *Light Scattering Spectra of Solids*, edited by G. B. Wright (Springer, Berlin, 1969), p. 369.

³J. A. Kash, S. S. Jha, and J. C. Tsang, Phys. Rev. Lett. **58**, 1869 (1987).

⁴B. H. Bairamov, I. P. Ipatova, V. A. Milorava, V. V. Toporov, K. Naukkarinen, T. Tuomi, G. Irmer, and J. Monecke, Phys. Rev. B **38**, 5722 (1988).

⁵B. H. Bairamov, V. A. Voitenko, I. P. Ipatova, V. K. Negoduyko,

and V. V. Toporov, Phys. Rev. B **50**, 14 923 (1994).

⁶E. T. M. Kernohan, R. T. Philips, B. H. Bairamov, D. A. Ritchie, and M. Y. Simmons, Solid State Commun. **100**, 263 (1996).

⁷D. von der Linde, J. Kuhl, and H. Klingenberg, Phys. Rev. Lett. **44**, 1505 (1980).

⁸J. A. Kash and J. C. Tsang, in *Spectroscopy of Nonequilibrium Electrons and Phonons*, edited by C. V. Shank and B. P. Zakharchenya (Elsevier, New York, 1992), p. 113.

⁹F. Vallée and F. Bogani, Phys. Rev. B **43**, 12 049 (1991).

¹⁰F. Vallée, Phys. Rev. B **49**, 2460 (1994).

¹¹W. E. Bron, J. Kuhl, and B. K. Rhee, Phys. Rev. B **34**, 6961 (1986).

- ¹²F. Ganikhanov and F. Vallée, *Phys. Rev. B* **55**, 15 614 (1997).
- ¹³A. Laubereau, D. von der Linde, and W. Kaiser, *Opt. Commun.* **7**, 173 (1973).
- ¹⁴G. M. Gale, F. Vallée, and C. Flytzanis, *Phys. Rev. Lett.* **57**, 1867 (1986).
- ¹⁵F. Vallée and C. Flytzanis, *Phys. Rev. B* **46**, 13 799 (1992).
- ¹⁶T. Juhasz and W. E. Bron, *Phys. Rev. Lett.* **63**, 2385 (1989).
- ¹⁷E. D. Grann, K. T. Tsen, and D. K. Ferry, *Phys. Rev. B* **53**, 9847 (1996).
- ¹⁸J. A. Kash, J. C. Tsang, and J. M. Hvam, *Phys. Rev. Lett.* **54**, 2151 (1985).
- ¹⁹R. A. Cowley, *J. Phys. (Paris)* **26**, 659 (1965).
- ²⁰P. G. Klemens, *Phys. Rev.* **148**, 845 (1966).
- ²¹A. Debernardi, S. Baroni, and E. Molinari, *Phys. Rev. Lett.* **75**, 1819 (1995).
- ²²A. Debernardi, *Phys. Rev. B* **57**, 12 847 (1998).
- ²³G. P. Srivastava, *The Physics of Phonons* (Hilger, Bristol, 1990).
- ²⁴B. K. Ridley and R. Gupta, *Phys. Rev. B* **43**, 4939 (1991).
- ²⁵S. Usher and G. P. Srivastava, *Phys. Rev. B* **50**, 14 179 (1994).
- ²⁶J. Menéndez and M. Cardona, *Phys. Rev. B* **29**, 2051 (1984).
- ²⁷V. Yu. Davydov, Yu. E. Kitaev, I. N. Goncharuk, A. N. Smirnov, J. Graul, O. Semchinova, D. Uffmann, M. B. Smirnov, A. P. Mirgorodsky, and R. A. Evarestov, *Phys. Rev. B* **58**, 12 899 (1998).
- ²⁸C. Bungaro, K. Rapcewicz, and J. Bernholc, *Phys. Rev. B* **61**, 6720 (2000).
- ²⁹H. M. Tütüncü and G. P. Srivastava, *Phys. Rev. B* **62**, 5028 (2000).
- ³⁰B. K. Ridley, *J. Phys.: Condens. Matter* **8**, L511 (1996).
- ³¹S. Barman and G. P. Srivastava, *Appl. Phys. Lett.* **81**, 3395 (2002).
- ³²*Landolt-Börnstein Numerical Data and Functional Relationships in Science and Technology*, Vol. 17, *Semiconductors*, edited by O. Madelung, M. Sculz, and H. Weiss (1982).
- ³³S. C. Miller and W. F. Love, *Tables of Irreducible Representations of Space Groups and Corepresentations of Magnetic Space Groups* (Pruett, Boulder, 1994).
- ³⁴R. J. Bruls, H. T. Hintzen, G. de With, R. Metselaar, and J. C. van Miltenburg, *J. Phys. Chem. Solids* **62**, 783 (2001).
- ³⁵K. T. Tsen, D. K. Ferry, A. Botchkarev, B. Sverdlov, A. Salvador, and H. Morkoc, *Appl. Phys. Lett.* **72**, 2132 (1998).
- ³⁶S. Tripathy, S. J. Chua, and A. Ramam, *J. Phys.: Condens. Matter* **14**, 4461 (2002).
- ³⁷L. Bergman, D. Alexson, P. L. Murphy, R. J. Nemanich, M. Dutta, M. A. Stroscio, C. Balkas, H. Shin, and R. F. Davis, *Phys. Rev. B* **59**, 12 977 (1999).
- ³⁸M. Kuball, J. M. Hayes, Ying Shi, and J. H. Edgar, *Appl. Phys. Lett.* **77**, 1958 (2000).
- ³⁹E. S. Zouboulis and M. Grimsditch, *Phys. Rev. B* **43**, 12 490 (1991).
- ⁴⁰H. M. Tütüncü, G. P. Srivastava, and S. Duman, *Physica B* **316**, 317, 190 (2002).
- ⁴¹H. Herchen and M. A. Cappelli, *Phys. Rev. B* **47**, 14 193 (1993).
- ⁴²D. J. Ecsedy and P. G. Klemens, *Phys. Rev. B* **15**, 5957 (1977).
- ⁴³G. Irmer, M. Wenzel, and J. Monecke, *Phys. Status Solidi B* **195**, 85 (1996).
- ⁴⁴P. H. Borchers, G. F. Alfrey, D. H. Saunderson, and A. D. B. Woods, *J. Phys. C* **8**, 2022 (1975).
- ⁴⁵H. M. Tütüncü and G. P. Srivastava, *Phys. Rev. B* **53**, 15 675 (1996).
- ⁴⁶B. D. Rajput and D. A. Browne, *Phys. Rev. B* **53**, 9052 (1996).